第26卷 第10期 半 导 体 学 报 Vol. 26 No. 10
2005年10月 CHINESE JOURNAL OF SEMICONDUCTORS Oct. ,2005

Theoretical Analysis of Gain and Threshold Current Density for Long Wavelength GaAs-Based Quantum-Dot Lasers *

Deng Shengling, Huang Yongzhen, Jin Chaoyuan, and Yu Lijuan

(State Key Laboratory on Integrated Optoelectronics, Institute of Semiconductors, Chinese Academy of Sciences, Beijing 100083, China)

Abstract: Quantum dot gain spectra based on harmonic oscillator model are calculated including and excluding excitons. The effects of non-equilibrium distributions are considered at low temperatures. The variations of threshold current density in a wide temperature range are analyzed and the negative characteristic temperature and oscillatory characteristic temperature appearing in that temperature range are discussed. Also, the improvement of quantum dot lasers' performance is investigated through vertical stacking and p-type doping and the optimal dot density, which corresponds to minimal threshold current density, is calculated.

Key words: quantum dot lasers; multiple energy levels; gain spectrum; temperature dependence

EEACC: 4320J; 4250; 2520

CLC number: TN302 **Document code:** A **Article ID:** 0253-4177(2005)10-1898-07

1 Introduction

For QDs lasers, gain characteristic is very important. It decides which and how many states participate in lasing and how threshold current changes with temperature. In previous calculation, carriers were generally treated either as free ones[1] or as excitons[2]. However, free carriers and excitons coexist all the time and neglecting either one may result in inaccurate modeling. To address this problem, a model was introduced that included both free carriers and excitons[3], and with which the author modeled T_0 (characteristic temperature) oscillation with cavity length. However, that work did not explain the T_0 oscillation of a given QDs laser with temperature, which was observed experimentally[4] and is much more meaningful. In this work, we will investigate the characteristics of gain and threshold currents of long wavelength QDs lasers in a wide temperature range. The effects of vertical stacking and p-doping on threshold currents are also considered.

2 Harmonic oscillator model

To obtain QD energy levels, we employed the harmonic oscillator model[5], as is illustrated in Fig. 1. This model takes into account QD's size variation and yields equally separated states. According to the model, electron energy spectrum is described as

$$\hbar\omega_{e,n} = \hbar\omega_{\perp,e}(n_x + n_y + 1) + \hbar\omega_{z,e}\left(n_z + \frac{1}{2}\right) \quad (1)$$

* Project supported by the National High Technology Research and Development Program of China (No. 2003AA311070) and the National Natural Science Foundation of China (No. 60225011)

Deng Shengling male, was born in 1979, master candidate. He is working in QD lasers.

Huang Yongzhen male, was born in 1963, professor. He is interested in research on semiconductor optoelectronics.

Yu Lijuan female, was born in 1963, associated professor. She is working in semiconductor devices.

Received 10 October 2004, revised manuscript received 17 March 2005

where n_x, n_y, and n_z denote the quantum numbers along x, y, and z directions, respectively, and n_x is equivalent to n_y. $\hbar\omega_{\perp,e}$ is the energy separation due to lateral confinement and $\hbar\omega_{z,e}$ is that due to vertical confinement. The hole energy spectrum $\hbar\omega_{h,n}$ has a similar form. For 1.3μm QDs, the average size is as large as 30nm in diameter and 11nm in height after covering[6]. The corresponding energy separations are 72meV and 11meV in conduction and valence band, which fit experimental data[7] well. There exist 3 states in conduction band and 6 in valence band.

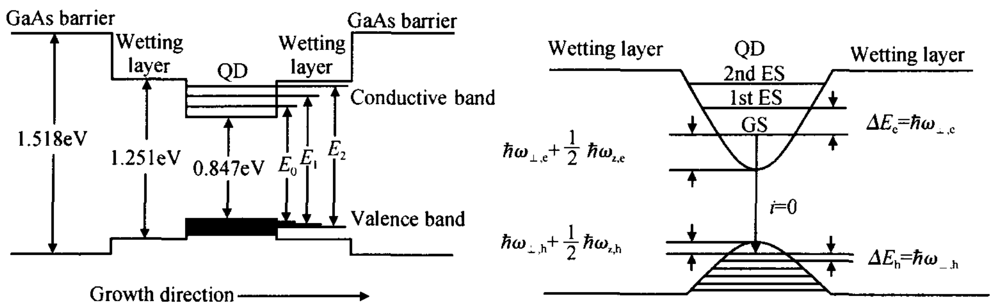

Fig. 1 Schematic illustration of the bands structure and transition in a QD

3 Carrier distribution and model gain

At relatively high temperatures, carriers in different QDs can couple through thermal emission into the wetting layer and the re-capture process. This coupling will establish a quasi-Fermi distribution and we call it equilibrium distribution here. At low temperatures, however, thermal escape is strongly suppressed and states population is only determined by capture probability of different-sized dots, and we call it non-equilibrium distribution. Since thermal emission relies heavily on temperature, it is reasonable to assume a boundary temperature T_B, which separates these two cases. Based on the calculation above, $k_B T$ will be smaller than the hole energy separation when $T < 130$ K, so we choose $T_B = 130$ K in this work.

The linear modal gain of QDs ensemble is given in Ref. [8] and it is commonly used in modeling. We modify it to adapt to the multiple-level situation as

$$g_{\mathrm{modal}}(E) = N_l \frac{\pi e^2 \hbar \Gamma n_{\mathrm{QD}}}{m_0^2 \varepsilon_0 c n_r z} \sum_{i=1}^{3} \frac{2 S_i}{E} \int |M_b|^2 |M_{\mathrm{env}}|^2 \times G(E', E_i)(f_e^c(E') - f_e^v(E')) L(E', E) \mathrm{d}E' \quad (2)$$

where M_b is the bulk matrix element and M_{env} is the wavefunction overlap. S_i is the ith transition degeneracy and N_l is the QDs layer number. $f_e^c(E)$ and $f_e^v(E)$ denote electrons' occupation probability in conduction and valence band. Gaussian distribution $G(E, E_i)$ represents inhomogeneous broadening resulting from QDs inequality with σ accounting for size and shape fluctuation.

$$G(E, E_i) = \frac{1}{\sqrt{2\pi}\sigma} \times \frac{1}{-2\sigma^2}(E - E_i)^2 \quad (3)$$

The Lorentzian

$$L(E', E) = \frac{1}{\pi} \times \frac{\Gamma_{\mathrm{in}}}{(E' - E)^2 + (\Gamma_{\mathrm{in}})^2} \quad (4)$$

describes the effect of homogeneous broadening. n_{QD} is the QDs' surface density and n_r is the refractive index. Γ/z denotes optical confinement factor normalized by active layer thickness.

In the following calculation, we choose $N_l = 2$, $\sigma = 20$meV, $n_{\mathrm{QD}} = 3 \times 10^{10}\,\mathrm{cm}^{-2}$, $n_r = 3.3$, and $\Gamma/z = 3.2 \times 10^6\,\mathrm{m}^{-1}$. As for Eq. (4), we replace it with a δ-function in the non-equilibrium case[9] and choose $\Gamma_{\mathrm{in}} = 6$meV in the equilibrium case.

3.1 Non-equilibrium distribution ($T < T_B$)

In this situation, it is a good approximation that carriers fill from the lowest energy level in each dot. Figure 2 shows the non-equilibrium gain spectrum. As a result of this unique filling pattern, the first excited state (ES1) modal gain remains minimum until the ground state (GS) saturates, and the same is true for ES2 and ES1. The GS saturated modal gain is 12.2cm^{-1} here.

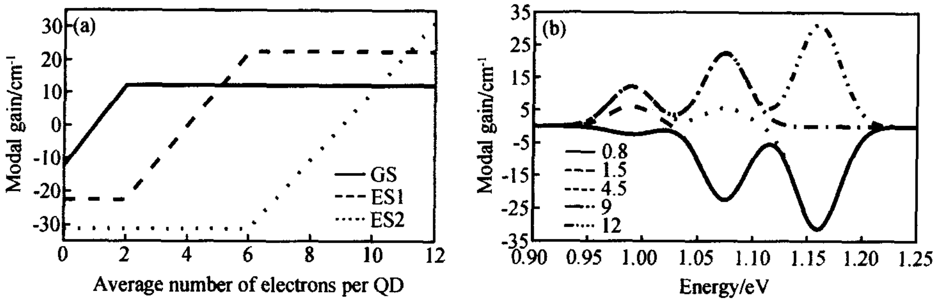

Fig. 2 (a) Non-equilibrium modal gain at center energy; (b) Non-equilibrium modal gain versus injection intensity

3.2 Equilibrium distribution ($T > T_B$)

In this situation, electrons' density relates to QDs' surface density through

$$n_e = \sum_{i=1}^{3} \int S_i n_{QD} G(E, E_i) f_e(E) \mathrm{d}E \qquad (5)$$

According to the relation of $n_e = \int \rho_e f_e(E) \mathrm{d}E$, electrons' effective density of states is

$$\rho_e = \frac{2 n_{QD}}{\sqrt{2\pi}\sigma} \sum_{i=1}^{3} S_i \exp\left(-\frac{1}{2\sigma^2}(E - E_i)^2\right) \qquad (6)$$

As Fig. 3 shows, with increasing σ, overlaps between different states become stronger, which will prevent carriers from concentrating into certain energy positions[10] and degrade device performance. Therefore, QDs with less size fluctuation is crucially important. Moreover, since ρ_e is proportional to n_{QD}, higher n_{QD} is also desired.

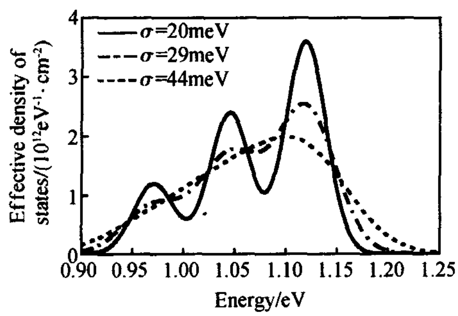

Fig. 3 QDs effective density of states versus different size fluctuations

Comparing Fig. 4 with Fig. 2, we find that the equilibrium saturated modal gain of each state is much lower than its counterpart in the non-equilibrium case. This is because lots of holes are emitted into higher states in the equilibrium case and the inversion factor $f_e^c(E) - f_e^v(E)$ is reduced.

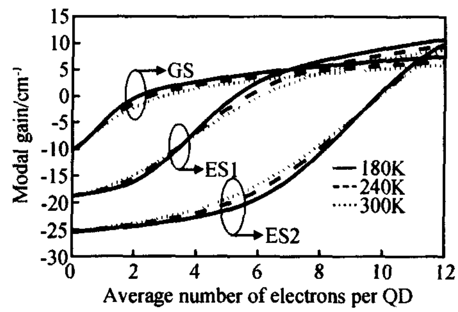

Fig. 4 Equilibrium modal gain at center energy

3.3 Excitons effect on gain spectrum

The above discussion is based on a free carriers' assumption. However, excitons and free carriers in fact exist in the QDs simultaneously. Because of strong QDs confinement and strong Coulomb interaction, excitons have much larger wavefunction overlaps. Moreover, in contrast to separate electron and hole quasi-Fermi levels, we assume excitons follow a uniform exciton Fermi level. These differences may have a remarkable influence on modal gain. A model[3] incorporating excitons influence can be shown as

$$g_{modal}(E) = g_{free}(E) n_{free} + g_{exciton}(E) n_{exciton} \qquad (7)$$

$$n_{exciton} = 1 - \sqrt{n_{exciton} \times \frac{1}{\exp\left(\frac{E_B}{kT}\right) - \left(1 + \frac{E_B}{kT}\right)}} \qquad (8)$$

where n_{free} and $n_{exciton}$ denote the ratios of free carriers and excitons. The binding energy E_B is chosen to be 20meV[2]. According to this model, GS saturated modal gain at 300 K is 15.7cm^{-1}, much larger than 5.2cm^{-1} of the free carriers case. Due to decreased excitons, threshold level will shift from GS to ES when temperature increases.

For non-equilibrium case, modal gain is affected by temperature similarly. This makes threshold current not completely independent of temperature, differing from predictions for ideal QDs lasers.

4　Characteristics of threshold current density

In the equilibrium regime, QDs couple through the wetting layer and the occupation of the wetting layer makes states population temperature-dependent. With rising temperature, more carriers will evaporate out of QDs. Therefore, we must include the wetting layer influence when considering current density.

$$J = N_1 \frac{q}{\eta_i} \times \left(\frac{n_w}{\tau_w} + \frac{n_{QD} N_a}{\tau_{QD}} \right) \tag{9}$$

where τ_w is the recombination time in the wetting layer, τ_{QD} is the average recombination time in QDs, N_a is the average carriers number per QD, and n_w is carriers' surface density in the wetting layer, which should be derived from steady-state rate equation, η is the injection efficiency.

For non-equilibrium case, thermal coupling is negligible, and Equation (9) can be simplified as

$$J = N_1 \frac{q}{\eta_i} \times \frac{n_{QD} N_a}{\tau_{QD}} \tag{10}$$

Equations (11) and (12) describe the threshold condition and threshold current's temperature dependence respectively

$$g_{modal} = \frac{1}{L} \ln\left(\frac{1}{R}\right) + \alpha_n \tag{11}$$

$$J_{th} = J_0 \exp(T/T_0) \tag{12}$$

We choose $\tau_w = 2$ns, $\tau_{QD} = 0.5$ns, and $\eta = 70\%$, the magnitude of which are widely used in modeling[3]. $R = 0.31$ is reflectivity of facets as cleaved and $\alpha_n = 2$cm^{-1} is after most recent experimental results. Figure 5 (a) shows the calculated J_{th} for QDs lasers with different cavity lengths. We find J_{th} changes only slightly at low temperatures while increases remarkably at high temperatures. The whole trend agrees with experimental results[5] very well.

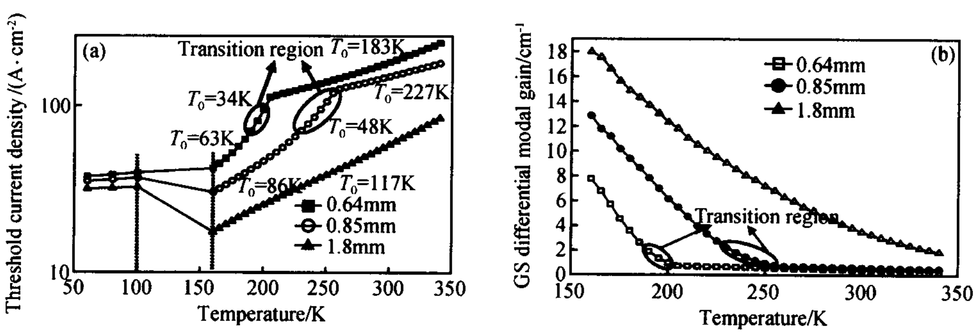

Fig. 5　(a) T_0 and J_{th} for QDs lasers with different cavity lengths; (b) GS differential modal gain at threshold level versus temperature

Due to higher losses, shorter cavity corresponds to higher J_{th}, but this is much more evident in the equilibrium regime. Also in this regime, T_0 changes not monotonously for the 0.64mm and 0.85mm lasers. Comparing Fig. 5 (a) with Fig. 5 (b), we find T_0 changes when threshold level shifts from GS linear region to ES1 linear region via GS saturated region. For the 0.64mm laser, this appears when temperature increases from 190 to 200 K; for the 0.85mm laser, this happens at a higher temperature range of 230～255 K. But for the 1.8mm one, such a transition does not appear up to 340 K. Near GS saturated region, T_0 decreases from 63 to 34 K for the 0.64mm laser and from 86 to 48 K for the 0.85mm one. In ES1 linear region, T_0 is 183 K for the 0.64mm laser and 227 K for the 0.85mm one, which is much larger than that in GS due to the higher differential gain of ES1. Such variations will appear repeatedly if temperature further increases and T_0 will exhibit oscillation characteristic. This phenomenon was firstly reported in Ref. [4]. We find it directly results from the excited states involvement.

At lower temperatures, J_{th} is rather insensitive to temperature. For example, T_0 is 677, 813, and 1324 K for the 0.64, 0.85, and 1.8mm lasers respectively. Such high T_0 agrees with experimental results[4] well. Around T_B, lasers undergo gradual changes from non-equilibrium distribution to equilibrium distribution and J_{th} decreases during the process. In Eq. (12), this corresponds to a negative T_0, as reported in Ref. [11]. Based on our calculation and analysis, it can be explained by QDs' equal occupation probability in the non-equilibrium regime, where carriers favor no particular energy, making saturated modal gain lower than that at temperatures immediately above T_B.

5 Improvement of QDs laser's performance

According to the above discussion, higher modal gain is desired for improving T_0 and lowering J_{th}. p-type doping[7,13] and vertical stacking[12], for instance, are feasible. The former measure increases GS inversion factor through enhancing GS hole occupation probability, while the latter increases the dot density in the active region. The results of these two approaches are shown in Fig. 6 (a) for the 0.85mm laser. Due to the increased modal gain, T_0 increases to 124 K and 145 K by stacking 4 and 8 layers respectively. Through doping 30 acceptors per dot, J_{th} reduces to be the lowest and J_{th}'s temperature stability is also ameliorated. For all the cases, the shift of threshold level from GS to ES1 is avoided.

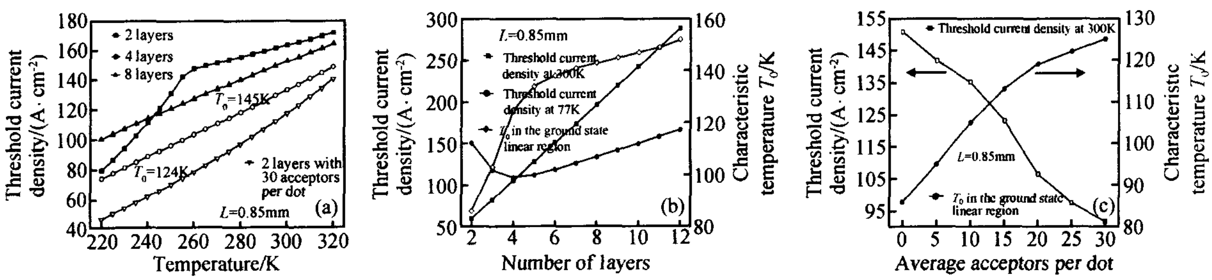

Fig. 6 (a) Variations of T_0 and J_{th}; (b) Influence of vertical stacking; (c) Influence of p-doping

However, because more QDs have to be pumped at the same time, carriers per dot are reduced, J_{th} will not necessarily decrease with more QDs layers. It is the competition outcome between carriers number per dot and QDs number that decides whether J_{th} increases or decreases. Seeing from Fig. 6(a), although J_{th} of the 4-layer structure remains smaller than that of the 2-layer one in the whole temperature range concerned, J_{th} of the 8-layer structure is larger than that of the 2-layer one below 240 K. Figure 6(b) shows the relation of J_{th}, T_0, and N_l at two typical temperature points. At 300 K, J_{th} declines as N_l increases from 2 to 4, but with still larger N_l, J_{th} begins to rise instead. At 77 K, however, J_{th} increases sharply with increasing layer. In GS linear region, T_0 improves evidently from 86 K of 2 layers to 124 K of 4 layers, but the improvement becomes much slower afterwards. Figure 6 (c) illustrates the influence of acceptors doped in the active region. Because p-doping does not increase QDs number, J_{th} will absolutely decrease. This is different from vertical stacking. Obviously, when acceptors increase from 10 to 15 per QD, the threshold level shifts to GS from ES1. For T_0, it keeps rising steadily from 86 K of undoped case to 108 K of 30 acceptors' case.

However, we must be aware of the concomitant negative effects. For example, stacking too many layers will spatially separate electrons and holes, lowering the direct recombination efficiency. Also, large amounts of acceptors will degrade the injection efficiency and increase the internal losses[7]. Therefore, in QDs laser design, all factors must be carefully balanced.

Figure 7 exhibits the relationship between J_{th} and n_{QD}. Undoubtedly, higher n_{QD} makes threshold condition easier to be met by GS, as is manifested in Eq. (2). For instance, when $N_l = 2$, n_{QD} has to surpass $4 \times 10^{10}\,cm^{-2}$, while for $N_l = 4$, this value reduces to $2 \times 10^{10}\,cm^{-2}$. However, there exists optimal n_{QD} corresponding to minimal J_{th}. Further increasing n_{QD} above this value continues to decrease carriers in a single dot but will lead to larger J_{th}. The reason for this characteristic is similar to the vertical stacking case.

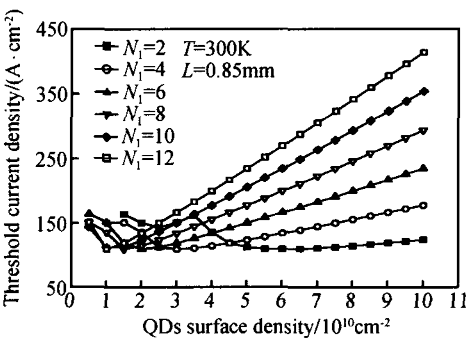

Fig. 7　J_{th} versus n_{QD} as N_l increases from 2 to 12

6　Conclusion

Gain spectrum strongly relies on temperature in the equilibrium regime. Deeply affected by this dependence, T_0 oscillates when temperature increases. Between non-equilibrium regime and equilibrium regime, T_0 is negative, which results from the different carrier distributions.

The existence of excited states may lead to many negative effects on QDs lasers performance. Through vertical stacking and p-type doping, we can limit the excited states influence, realize GS operation, increase T_0, and lower J_{th}.

References

[1] Asryan L V, Grundmann M, Ledentsov N N, et al. Effect of excited-state transitions on the threshold characteristics of a quantum dot laser. IEEE J Quantum Electron, 2001, 37: 418

[2] Bimberg D, Grundmann M, Ledentsov N N. Quantum dot heterostructures. Chichester, New York: John Wiley, 1999

[3] Dikshit A A, Pikal J M. Carrier distribution, gain, and lasing in 1.3-μm InAs-InGaAs quantum-dot lasers. IEEE J Quantum Electron, 2004, 40: 105

[4] Chang C A, Hwang F C, Wu Z R, et al. Oscillatory characteristic temperature of InAs quantum-dot laser. IEEE Photonics Technol Lett, 2001, 13: 915

[5] Park G, Shchekin O B, Deppe D G. Temperature dependence of gain saturation in multilevel quantum dot lasers. IEEE J Quantum Electron, 2000, 36: 1065

[6] Krishna S, Zhu D, Xu J, et al. Structural and luminescence characteristics of cycled submonolayer InAs/GaAs quantum dots with room-temperature emission at 1.3μm. J Appl Phys, 1999, 86: 6135

[7] Shchekin O B, Deppe D G. 1.3μm InAs quantum dot laser with T_0 = 161 K from 0 to 80 ℃. Appl Phys Lett, 2002, 80: 3277

[8] Bimberg D, Kirstaedter N, Ledentsov N N, et al. InGaAs-GaAs quantum-dot lasers. IEEE J Sel Topics Quantum Electron, 1997, 3: 196

[9] Sauvage S, Boucaud P, Brunhes T, et al. Dephasing of intersublevel polarizations in InAs/GaAs self-assembled quantum dots. Phys Rev B, 2002, 66: 153312-1

[10] Ning Yongqiang, Gao Xin, Wang Lijun, et al. Spontaneous emission and optical gain in InGaAs quantum dots. Chinese Journal of Semiconductors, 2002, 23(4): 373 (in Chinese) [**宁永强, 高欣, 王立军, 等. InGaAs 量子点的自发发射及光增益. 半导体学报**, 2002, 23(4): 373]

[11] Zhukov A E, Ustinov V M, Egorov A Y, et al. Negative characteristic temperature of InGaAs quantum dot injection laser. Jpn J Appl Phys, 1997, 36: 4216

[12] Grundmann M, Bimberg D. Gain and threshold of quantum dot lasers: theory and comparison to experiments. Jpn J Appl Phys, 1997, 36: 4181

[13] Shchekin O B, Ahn J, Deppe D G. High temperature performance of self-organized quantum dot laser with stacked p-dope active region. Electron Lett, 2002, 38: 712

GaAs 基长波长量子点激光器增益和阈值电流密度的理论分析*

邓盛凌　黄永箴　金潮渊　于丽娟

(中国科学院半导体研究所 集成光电子学国家重点实验室, 北京　100083)

摘要: 基于谐振子模型的量子点能级,计算了包括和排除激子影响时多能级的增益谱. 考虑了低温时非平衡载流子分布. 得出了较宽温度范围内阈值电流密度的变化,包括负温度及振荡温度效应. 研究了垂直层叠和 p 型掺杂对量子点激光器性能的改善,并讨论了获得极小阈值电流密度时的最佳量子点密度.

关键词: 量子点激光器; 多能级; 增益谱; 温度依赖

EEACC: 4320J; 4250; 2520

中图分类号: TN302　　**文献标识码**: A　　**文章编号**: 0253-4177(2005)10-1898-07

* 国家高技术研究发展计划(批准号:2003AA311070)和国家自然科学基金(批准号:60225011)资助项目

邓盛凌　男,1979 年出生,硕士研究生,主要从事量子点激光器研究.

黄永箴　男,1963 年出生,研究员,主要从事半导体光电子学研究.

于丽娟　女,1963 年出生,副研究员,主要从事半导体材料和器件研究.

2004-10-10 收到,2005-03-17 定稿